Electrostatic Interactions in Asymmetric Organocatalysis

Rajat Maji, Sharath Chandra Mallojjala, and Steven E. Wheeler*

Department of Chemistry, University of Georgia, Athens, GA 30602
E-mail: swheele2@uga.edu

Abstract

Electrostatic interactions are ubiquitous in catalytic systems and are often decisive in determining reactivity and stereoselectivity. However, a lack of understanding of the fundamental underlying principles has long stymied our ability to fully harness the power of these interactions. Fortunately, advances in affordable computing power together with new quantum chemistry methods have increasingly enabled a detailed atomic-level view. Empowered by this more nuanced perspective, synthetic practitioners are now adopting these techniques with growing enthusiasm. In this review, we narrate our recent results rooted in state-of-the-art quantum chemical computations, describing pivotal roles for electrostatic interactions in the organization of transition state (TS) structures to direct reactivity and selectivity in the realm of asymmetric organocatalysis. To provide readers with a fundamental foundation in electrostatics, we first introduce a few guiding principles, beginning with a brief discussion of electrostatic interactions and electrostatics-dominated non-covalent interactions as well as and their modulating factors. We then describe computational approaches to capture these effects, primarily through representative case studies. Subsequently, we cover some general strategies that have been utilized to impart stereocontrol in asymmetric organocatalysis, presenting our own results along with selected highlights from other groups.

We then briefly cover our most significant recent computational investigations in three specific branches of asymmetric organocatalysis, beginning with chiral phosphoric acid (CPA) catalysis. We disclose how CPA-catalyzed asymmetric ring openings of *meso*-epoxides are driven by stabilization of a transient partial positive charge in the S_N2-like TS by the chiral electrostatic environment of the catalyst. We also report on substrate-dependent electrostatic effects from our study of CPA-catalyzed intramolecular oxetane desymmetrizations. For non-chelating oxetane substrates, electrostatic interactions with the catalyst confers stereoselectivity, whereas oxetanes with chelating groups adopt a different binding mode that overrides this electrostatic stereodetermination and erodes selectivity. In another example, computational approaches revealed a pivotal role of CH···O and NH···O hydrogen bonding in CPA-catalyzed asymmetric synthesis of 2,3-dihydroquinazolinones. These interactions control selectivity during the enantiodetermining intramolecular amine addition step, and their strength is modulated by substrate positioning within the electrostatic environment created by the catalyst, allowing us to rationalize the effect of introducing *o*-substituents. Next, we describe our efforts to understand selectivity

in a series of NHC-catalyzed kinetic resolutions. We discovered that electrostatic interactions are the common driver of selectivity. Finally, we discuss our breakthrough in understanding asymmetric silylium ion-catalyzed Diels–Alder cycloaddition of cinnamate esters to cyclopentadienes. The diastereoselectivity of these transformations is guided by CH···O electrostatic interactions that selectively stabilize the *endo*-transition state. Additionally, we deduced the geometry of the preferred binding mode to explain the requirement for a 9-fluorenylmethyl ester to achieve high selectivity.

We conclude with a brief overview of the outstanding challenges and the potential roles of computational chemistry in enabling the exploitation of electrostatic interactions in asymmetric organocatalysis.

KEY REFERENCES

- Maji, R.; Ugale, H.; Wheeler, S. E. Understanding the Reactivity and Selectivity of Fluxional Chiral DMAP-Catalyzed Kinetic Resolutions of Axially Chiral Biaryls. *Chem. Eur. J.* **2019**, *25*, 4452–4459.[1] This work captures the effect of electrostatic interactions in controlling the reactive conformation in chiral nucleophilic catalysis.

- Maji, R.; Champagne, P. A.; Houk, K. N.; Wheeler, S. E. Activation Mode and Origin of Selectivity in Chiral Phosphoric Acid-Catalyzed Oxacycle Formation by Intramolecular Oxetane Desymmetrizations. *ACS Catal.* **2017**, *7*, 7332–7339.[2] This paper describes the importance of a substrate-dependent electrostatic effects in controlling the selectivity in chiral phosphoric acid-catalyzed reactions.

- Maji, R.; Wheeler, S. E. Importance of Electrostatic Effects in the Stereoselectivity of NHC-Catalyzed Kinetic Resolutions. *J. Am. Chem. Soc.* **2017**, *139*, 12441–12449.[3] This publication displays the importance of electrostatic stabilization in NHC-catalyzed kinetic resolutions and the role of protic additives.

- Seguin, T. J.; Wheeler, S. E. Stacking and Electrostatic Interactions Drive the Stereoselectivity of Silylium-Ion Asymmetric Counteranion-Directed Catalysis. *Angew. Chem. Int. Ed.* **2016**, *55*, 15889–15893.[4] This work highlights the importance of the heterogenous electrostatic effect in controlling the diastereoselectivity in asymmetric silylium-based, counteranion-catalyzed Diels–Alder reactions.

1. Introduction

The last decade has seen considerable advancement in our understanding and appreciation of electrostatic interactions in organic systems. These interactions are pivotal in many stereoselective transformations, yet persistent knowledge gaps and misconceptions[5] prevent us from harnessing their full potential, particularly relating to their physical underpinnings and modulation. Nevertheless, enormous strides in computational chemistry have facilitated a growing understanding of how subtle changes in electrostatic interactions can impact everything from conformation to reactivity and stereoselectivity, enabling the development of improved catalysts and even new reactions. Other reviews[6, 7–8] have addressed various critical aspects of electrostatic interactions in reactions, including cation–π and anion–π interactions, CH···O hydrogen bonding, electrostatic catalysis, and biocatalysis. In this review, we offer a brief primer on electrostatically driven noncovalent interactions and chronicle our journey in this area over the past decade, including selected examples from other groups while highlighting outstanding challenges. We particularly consider our contributions to elucidating physical

aspects of electrostatic interactions, emphasizing the fundamental principles underlying electrostatic stabilization or destabilization, as illustrated through organocatalytic reactions where they contribute critically.

We begin by introducing electrostatic interactions and the factors that determine their strength, and then outline the various computational approaches used to study them in organocatalysis, illustrating their application through relevant examples with different modes of electrostatically mediated stereoinduction. Building on these methods and principles, we narrate findings from our group spanning three branches of organocatalysis. Subsequently, we document examples where in-depth knowledge of electrostatic interactions has facilitated rational design of catalysts and reactions, and then conclude by drawing attention to some outstanding challenges.

2. Brief Overview of Electrostatically Driven Interactions and their Modulators

"Electrostatic interaction" refers to the Columbic interaction of fixed charge distributions. This could include charge-charge, charge-dipole, dipole-dipole, etc. interactions. While the characterization of electrostatic interactions in molecular systems typically relies on quantum chemical methods (*e.g.*, density functional theory) to derive electron distributions within molecules, the electrostatic interactions themselves are purely classical in nature and therefore straightforward to understand. Regardless, Herbert[5] has recently reviewed some of the persistent misconceptions concerning electrostatic interactions in non-covalent interactions.

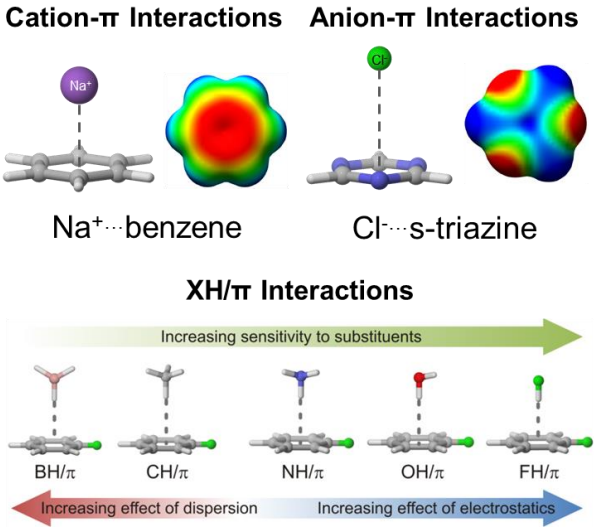

Figure 1. Examples of electrostatically-driven non-covalent interactions.

In addition to more general electrostatic interactions between charges, many "named" noncovalent interactions have significant electrostatic components (see Figure 1). Perhaps the most obvious examples are cation–π and anion–π interactions, which are attractive interactions between atomic or polyatomic cations and anions and the face of an aromatic ring, respectively. The strength of these and many other non-covalent interactions involving aromatic rings can be tuned over a considerable range by modulating the electrostatic potential (ESP) of the aromatic rings through the introduction of substituents[8] and/or heteroatoms.[9, 10] For instance, whereas benzene will not bind anions, s-triazine will. However, while it is common to ascribe changes in the ESP above the face of an arene to changes in the distribution or density of π-electrons, computations do not support this. Instead, we have shown[11] that the dominant effect of substituents on the ESPs of arenes is through space, not through π-resonance. Similarly, the dramatic effect of heteroatoms on arene ESPs are not due to the π-electrons but instead arise from the rearrangement of charges within the molecular plane.[9]

Hydrogen bonds are another important class of electrostatically-driven noncovalent interactions, including conventional cases such as OH···O and NH···O hydrogen bonds but also non-classical CH···O interactions.[12] Nature famously exploits these interactions for electrostatic stabilization within enzyme active sites by creating highly heterogeneous electrostatic pockets that stabilize high-energy intermediates (*e.g.*, tetrahedral intermediates, enolates) through formation of strong hydrogen bonding networks involving nearby atoms.[13] Another example is the XH/π interaction, which can describe the interaction between any X–H bond and the face of an arene. These interactions become increasingly driven by electrostatic effects as the electronegativity of X increases, meaning that their strength is increasingly sensitive to the electrostatic character of the arene. For instance, OH/π and FH/π interactions are dominated by electrostatics and exhibit strong effects due to substituents on the arene, whereas CH/π interactions are driven mainly by dispersion effects and tend to be insensitive to substituents. Among CH/π interactions, the degree of electrostatic character depends further on the hybridization of the carbon due to the increase in electronegativity with increasing *s*-character. That is, while alkynyl CH/π interactions exhibit some sensitivity to substituents and other changes in the arene, alkyl CH/π interactions do not.

In general, electrostatic interactions are maximized in the gas phase and in solution they become weaker as solvent polarity increases. Consequently, solvent can influence the outcome of electrostatically governed reactions in two distinct, but intertwined, ways: by affecting the

strength of electrostatic interactions and by determining the propensity for ion pairing. Systems with net charge on one or more interacting species exhibit the most dramatic effects, with exceptionally strong electrostatic interactions. For instance, the gas-phase binding energy of $CH_4\cdots OH^-$ is an order of magnitude stronger than that of the corresponding neutral complex, $CH_4\cdots OH_2$. Scheiner and coworkers[14] examined the impact of positive charge on many noncovalent interactions and provided rationale for the remarkably strong CH···O interactions in $R_3N^+C–H\cdots O=C$ complexes, a common recognition motif in stereoselective phase transfer catalysis.

3. Computational Tools to Probe Electrostatic Interactions in Catalysis

There are numerous computational approaches available to quantify electrostatic interactions. Chief among these are computed electrostatic potentials (ESPs), which are typically depicted as colored maps superimposed onto electron density isosurfaces (see examples of benzene and triazine in Figure 1). In these familiar plots, each point on the molecular surface is colored according to its ESP value. Regions with negative ESP (typically colored red) will stabilize electrostatic interactions with positive charges, whereas positive ESP regions (typically blue) will stabilize negative charges. Dougherty and coworkers[15] established the utility of ESP plots for qualitative and quantitative prediction and analysis of cation–π interactions and graphical ESP representations have proved invaluable for modelling and understanding electrostatically driven noncovalent interactions. However, it is important to remember that the electrostatic interaction between two molecules is not given by the interaction of their respective ESPs! Instead, one must consider the distribution of charges (typically approximated as atomic partial charges) of one molecule interacting with the ESP due the other molecule at the positions of these charges. Thus, we have found it far more fruitful to plot the ESP of one molecule in one or more planes containing key charged atoms of the other molecule (*e.g.*, see Figure 2b). One can go further and quantify electrostatic interactions as the sum of the product of partial atomic charges of one molecule with the ESP of the other molecule evaluated at these positions. The results from such analysis will depend somewhat on the choice used to devise the atomic partial charges, but in general provides a reasonable estimate of electrostatic interactions with the further benefit of providing atomic-level detail.

More qualitatively, molecular dipole and quadrupole moments are often computed and used to rationalize inter and intramolecular non-covalent interactions. While such analyses can

be useful, *local* multipole moments are generally more important for understanding close-contact interactions than the molecular values. For example, while a symmetric molecule like *para*-benzoquinone has no molecular dipole, the large local dipoles associated with each carbonyl group can engage in strong electrostatic interactions with other nearby molecules. This becomes increasingly important for larger molecules, since the interactions of molecular multipole moments become an increasingly poor predictor of electrostatic interactions as the size of the interacting molecules become increasingly larger than the distance between molecules.

Other more specialized tools are available that can be used to quantify different electrostatic interactions. For example, Bader's theory of atoms-in-molecules (AIM) provides a way to quantify polar interactions.[16] Cheng, Houk, and coworkers[17] used AIM to understand stereodifferentiation in squaramide-catalyzed asymmetric Michael addition of indoles to α-ketophosphonates, identifying an additional stabilizing CH···O interaction in the transition state (TS) leading to the major stereoisomer. Natural bond orbital (NBO) analysis is another widely used technique for quantifying interactions from an orbital perspective. For instance, Dudding and coworkers used NBO to explain the preferred substrate binding mode and origin of stereoselectivity in an organocatalyzed aza-Henry reaction.[18] The preferred alignment between the aldimine and catalyst is dictated by a homonuclear charge-assisted hydrogen bond (CAHB) that maximizes interaction energy, relative to an alternative conformation without it. The stereoselectivity correlated with the NCCN dihedral angle of the reacting substrates, with NBO analysis revealing a favored synclinal alignment of the TS enabling superior secondary orbital interaction between reactants. Finally, symmetry adapted perturbation theory (SAPT)[19] can provide robust predictions of interaction energies for nonbonded complexes and further decompose these energies into physically meaningful components, including electrostatic interactions. We used SAPT to understand the fluxionality of chiral DMAP-catalyzed kinetic resolutions (*vide infra*).[1] Atomic-SAPT (A-SAPT)[20] and functional group-SAPT (F-SAPT)[21] provide further opportunity to quantify electrostatic (and other) interactions at the group of individual atoms and functional groups, as demonstrated by Bakr and Sherrill[22] in their analysis of electrostatic control in the enantioselective addition of allyl and allenyl organoboron reagents to fluorinated ketones.[23]

Practitioners must be aware that the above methods all have limitations and can be sensitive to the system under study. Thus, it is desirable to quantify interactions using several different methods to properly validate conclusions. For example, we relied on multiple

techniques to understand the selectivity of *N*-heterocyclic carbene (NHC)-catalyzed kinetic resolution (KR) of cyclic diols,[3] including a fragmentation approach and subsequent quantification using AIM, NBO, and direct estimation of electrostatic stabilization through computed ESPs and partial charges.

4. Modes of Electrostatic Stabilization and Destabilization in Catalysis

Armed with knowledge of electrostatic interactions and techniques for their quantification, we will now investigate the prevailing modes by which these interactions impart control in catalysis through relevant examples. In general, electrostatic interactions can impact reactivity, through the lowering of the overall reaction barrier, or selectivity, by increasing the free energy difference between competing TS structures. While the roles of cation–π and anion–π interactions in chemical catalysis are extensively documented,[6,7] we mention two studies from our group.

First, our work on Matile's anion-π-catalyzed Kemp elimination[24] (reaction 1, Figure 2) highlighted the importance of quantifying the role non-covalent interactions in both the reactant and TS structure.[25] In this model reaction, the deprotonation of a nitrobenzoxazole by a catalytic base triggers a ring opening and formation of the cyanophenolic product. By engineering this reaction to occur over the face of a naphthalene diimine (NDI) through the use of a tethered carboxylate (**1**, Figure 1b), Matile demonstrated[24] the feasibility of using anion-π interactions to achieve rate acceleration. The rate of this reaction will depend on the free energy difference between the transition state (**TS**) and the catalyst substrate complex (**CS**). We showed that anion-π interactions are operative in both **CS** and **TS**. In the former, the anion is localized on the carboxylate, whereas in the latter it is delocalized across the substrate. More importantly, quantification of these anion-π interactions revealed that they were more stabilizing in **CS** than in **TS** (see Figure 2c), meaning that the net result of anion-π interactions was an overall increase in the reaction barrier. In other words, we found that while **1** undoubtedly catalyzes reaction 1, anion-π interactions were not responsible for the observed rate acceleration. This can be further understood by considering the ESP due to the NDI in the plane of the carboxylate and substrate (see Figure 2b). Going from **CS** to **TS**, the negative charge moves from one region of positive ESP to another. While a positive ESP indicates stabilization of negative charge, because the ESP is uniformly positive across this region the electrostatic stabilization of the negative charge is roughly equal regardless of whether it is centered on the carboxylate or delocalized onto the

substrate. While we did not find evidence of anion-π-induced barrier lowering for **1**, we devised a modified catalyst (**2**) for which we predict significant rate acceleration that can be attributed to anion-π interactions. By introducing an ethynyl linkage, the carboxylate is shifted to a region above the periphery of the NDI that has a more negative ESP. This effect is enhanced by moving on of the nitrile groups. The result is that there is now a strong electrostatic driving force for the migration of negative charge from the carboxylate to the substrate. This can be seen quantitatively in Figure 2d. For **2**, anion-π interactions of both the substrate and carboxylate are more favorable in TS and CS, resulting in significant lowering of the energy barrier.

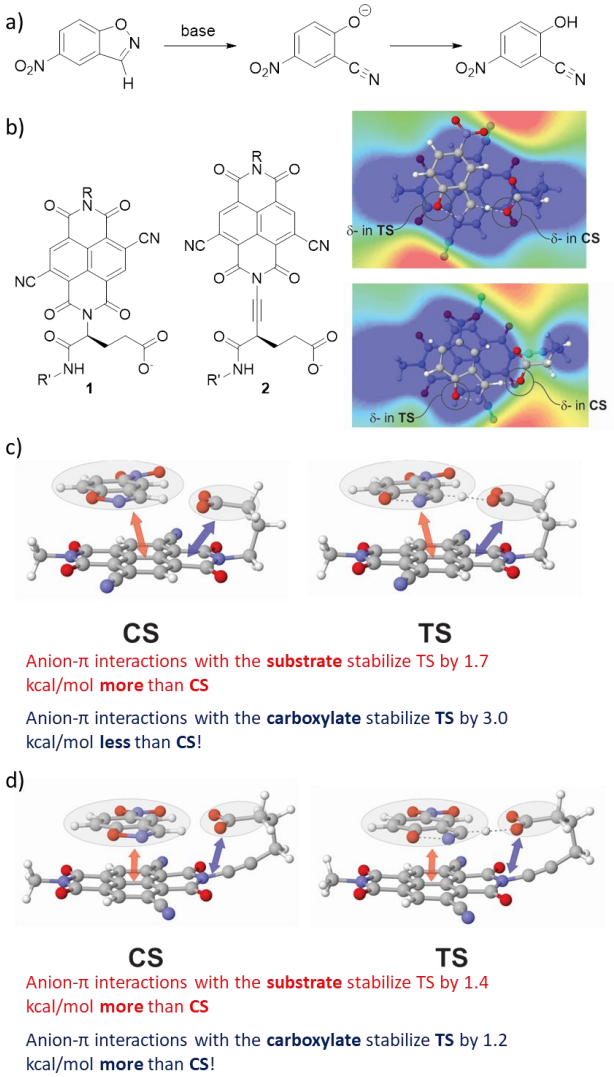

Figure 2. a) Kemp elimination studied by Matile and co-workers; b) Original anion-π catalyst from Matile *et al.*[24] (**1**) and redesigned catalyst from Lu and Wheeler25 (**2**) along with the ESPs due to the NDI component of the catalysts in the plane of the catalytic base and substrate for **1** (top) and **2** (bottom); c) and d) summary of the quantification of anion-π interactions in **CS** and **TS** for **1** and **2**, respectively. Portions adapted with permission from Ref. 25.

As a second example, we identified[1] a central role of cation–π interactions in the structural organization of DMAP catalysts for the kinetic resolution of axially chiral biaryls developed by Sibi *et al*.[26] (reaction 2, Figure 3). Although Sibi and coworkers[26] suggested that these catalysts are fluxional, we showed that the fluxionality in the ground state is lost during the reaction. Torsional analysis indicated that the *N*-acyl derivative formed during the catalytic cycle is very rigid, displaying conformational bias toward a geometry that favors stacking that leads to a sandwich-like structure (see Figure 3X). According to SAPT, this conformational bias stems from strong cation–π interactions that overpower the intrinsic angular strain. Thus, electrostatic stabilization not only overrides the inherent conformational preference of the acylated catalyst, but also directs the facial approach of alcohols to enhance stereoselectivity.

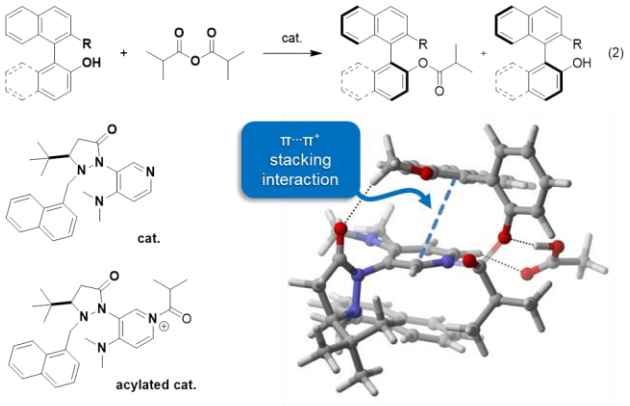

Figure 3. DMAP-catalyzed kinetic resolution of biaryls from Sibi *et al*.[26] along with the major TS structure showing the rigidfying π+-π stacking interaction. Portions adapted with permission from Ref. 1

Electrostatic interactions of isolated charges are another common stereodetermining factor. In their analysis of phase-transfer-catalyzed asymmetric cinchoninium ion alkylations, de Freitas Martins and Pliego[27] argued that electrostatic interactions between the departing chloride anion and the cationic cinchoninium nitrogen center stabilize the major TS via a CH···Cl hydrogen bond involving a benzylic hydrogen of the *N*-(*p*-trifluorobenzyl) group. The closer the chloride anion to the nitrogen center in the TS, the greater the stabilization, as supported by strong correlation of the Cl–N distance with $\Delta G^{\ddagger}$. This electrostatic model explained why changing the alkylating agent from methyl chloride, to bromide, to iodide, leads to decreased enantioselectivity through progressively weaker TS electrostatic stabilization.

Important electrostatic interactions can also stem from permanent or transient partial charges. We demonstrated[28] beneficial electrostatic stabilization in bipyridine *N*-oxide catalyzed asymmetric allylations (reaction 3, Figure 4). In particular, the stereoselectivity of these reactions was attributed to through-space electrostatic interactions of a chloride ligand (bound to *Si*) with both the formyl CH of the aldehyde and the vinyl CH of the allyl group in the TS leading to the major product. In the disfavoured TS structure these two H-atoms are directed away from the chlorines. This electrostatic model also explains the relatively poor stereoselectivity of the analogous *N*-oxide catalyzed propargylations (reaction 4), since the crucial vinyl hydrogen from the allylation case is absent.[29] An example of stereoinduction through the electrostatic stabilization of transient charges was provided by the Schedit and Cheong groups while studying an NHC-catalyzed dynamic kinetic resolution.[30] In the major TS for an intramolecular Aldol lactonization, the pyranyl C–H is positioned between the enolate oxygen and the incoming electrophilic carbonyl, stabilizing the developing negative charges via nonclassical CH···O hydrogen bonding.

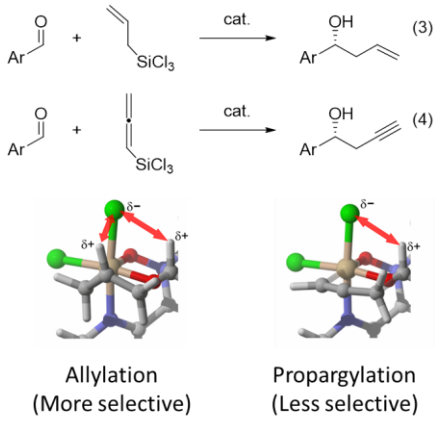

Figure 4. In stereoselective *N*-oxide catalyzed allylations (3) and propargylations (4) of aromatic aldehydes, the favored TS structure always features favorable electrostatic interactions between the formyl CH of the aldehyde and one of the Cl atoms bound to Si. The enhanced selectivity of allylations benefit from an additional $CH^{\delta+}\cdots{}^{\delta-}Cl$ interaction of the vinyl CH of the allyl group. Portions adapted from Ref. 29.

Akin to enzymes, small-molecule catalysts can also create stabilizing "oxyanion holes," typically by strategic placement of polar N–H and O–H groups within a conformationally rigid framework. For example, Wong and co-workers[31] recognized such effects in their study of *Cinchona* alkaloid-catalyzed cyclic anhydride desymmetrization. DFT analysis supported a three-point interaction model for stereoselectivity, where an oxyanion hole preferentially

stabilizes the TS for the major stereoisomer within the catalyst cavity through a C–H···O hydrogen bonding interaction involving a methoxy group on the catalyst. Analogous TS stabilization was documented by Papai, Soos, and coworkers[32] in their report on a bifunctional squaramide-catalyzed Michael addition.

Finally, we note that while stabilizing electrostatic interactions are often emphasized, electrostatic repulsion can equally direct selectivity. For example, Schoenebeck and coworkers[33] pinpointed a repulsive C=O···π interaction as the primary selectivity driver in NHC-catalyzed α,β-unsaturated acylazolium annulations. Based on computational analysis, they argued that the reaction proceeds via an oxyanion intermediate that is destabilized for the minor isomer due to electrostatic repulsion between a negatively polarized β-oxygen in the enolate and the π-cloud of the catalyst aryl group.

5. Electrostatically Driven Organocatalyzed Reactions

Below, we summarize our key recent findings revealing a central role for electrostatics in three popular types of asymmetric organocatalysis.

5.1 The Electrostatic Embrace in Chiral Phosphoric Acid-Catalyzed Reactions

We have contributed significantly to understanding the origins of stereoinduction in chiral phosphoric acid (CPA)-catalyzed reactions.[2, 34, 35] Over the last decade, CPAs have become widely used organocatalysts.[36] While conventional stereoselectivity explanations invoke steric factors, including shape complementarity of the chiral binding pocket, computational studies have offered a more nuanced picture wherein stereocontrol often hinges on a rich interplay of attractive and repulsive noncovalent interactions. Given the focus of this review, we will highlight examples where electrostatic effects predominate.

The importance of electrostatics in CPA catalysis has, in fact, been echoed multiple times in computational studies, with additional experimental support from Gschwind and coworkers.[37] Electrostatic stabilization by CPAs relies in many cases on their ability to engage substrates via classical (OH···X and NH···O) or nonclassical (CH···O) hydrogen bonds. The chiral binding pocket of CPAs offers a highly heterogeneous electrostatic environment, and we have found that the selectivity of some reactions can be understood based on the placement of key charged atoms of the substrate within this environment. Our first significant discovery in this area involved CPA-catalyzed asymmetric epoxide ring openings from Sun *et al*[38] (reaction 5, Figure 5) We

found that the narrow binding pocket resulted in the substrate adopting nearly identical orientations in the TS structures leading to the major and minor stereoisomers. As a result, there is a CH···O hydrogen bond in both TS structures. However, for the major TS this interaction involves the CH undergoing nucleophilic attack, which is not the case for the minor TS. Due to the build-up of significant positive charge on this CH group during the reaction, the major TS enjoys significantly more electrostatic stabilization through the interaction with the phosphoryl oxygen of the catalyst. Viewed another way, the narrow binding pocket of the catalyst positions the two epoxide carbons in different electrostatic environments, leading to a strong preference for nucleophilic attack of one over the other.

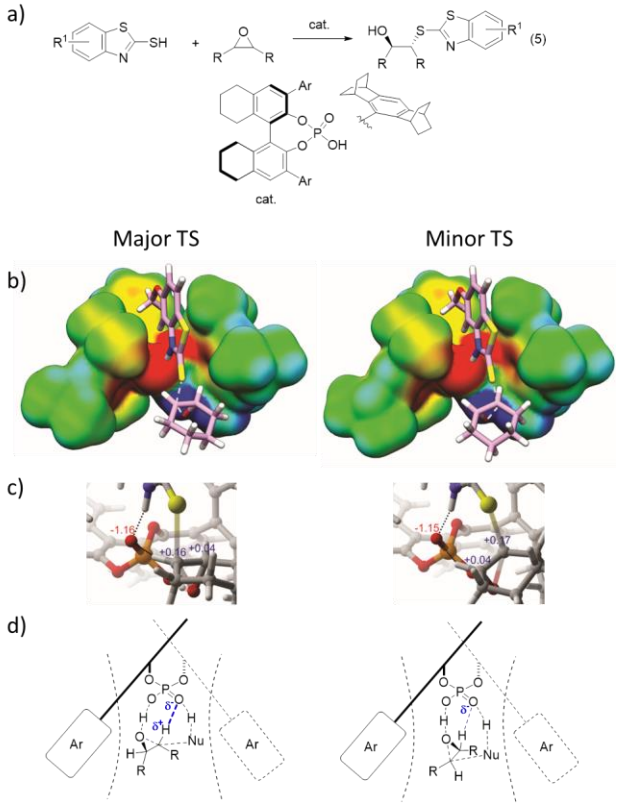

Figure 5. a) CPA catalyzed asymmetric ring-openings of cyclohexane oxide. b) TS structures leading to the major and minor stereoisomers. The ESP of the catalyst is shown along with the substrates (as sticks); c) NPA charges of key atoms; d) resulting stereochemical model. Portions adapted from Ref. 39.

We subsequently observed contrasting substrate-dependent electrostatic influences on intramolecular oxetane desymmetrizations (reaction 6, Figure 6).[2] For oxetanes with non-chelating groups (R = Me), superior selectivity was attributed to differences in the electrostatic interactions between the phosphate of the catalyst and the α-C–H of the oxetane that favour the

TS for formation of the major stereoisomer. In contrast, introducing a chelating group (R = OH) induces a different binding mode where the resulting net electrostatic stabilization favors the minor stereoisomer and erodes selectivity.

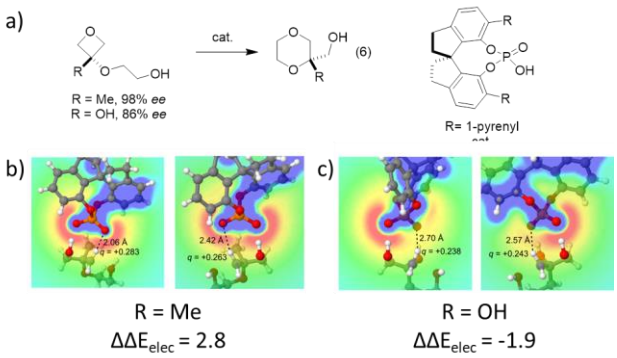

Figure 6. a) CPA catalyzed intramolecular oxetane desymmetrization; b) and c) quantifying the elelectrostatic controbution to the energy difference between the minor and major stereocontrolling TS structures ($\Delta\Delta E_{elec}$, in kcal/mol)**.** Portions adapted with permission from Ref. 2.

Finally, while exploring the origin of enantioselectivity in catalytic asymmetric synthesis of 2,3-dihydroquinazolinones using SPINOL-derived CPAs, we similarly identified a pivotal role for hydrogen bonds with the phosphate group of the catalyst whose strength varies depending on substrate positioning within the electrostatic environment of the catalyst.[35] The enantiodetermining intramolecular amine addition step was analyzed computationally for twelve different reactions, giving excellent agreement with experiment. Introducing *o*-substituents preferentially enhanced NH···O and CH···O interactions in one TS over the other, allowing the major isomer to be rationalized in terms of both electrostatics and geometry (reaction 7, Figure 7). The strength of these interactions is modulated by their position within the electrostatic environment created by the catalyst, establishing the feasibility of precisely controlling selectivity in organocatalyzed reactions by tuning electrostatic interactions.

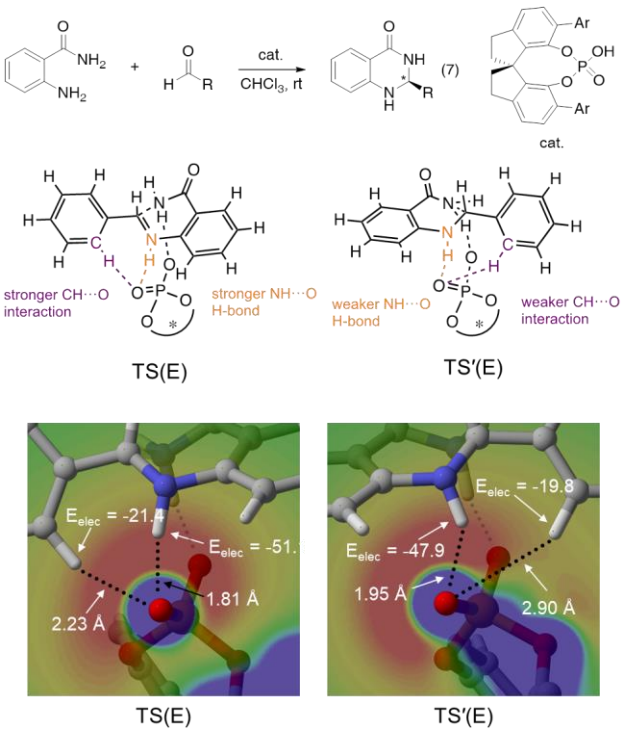

Figure 7. Electrostatic modulation of a SPINOL-derived CPA-catalyzed synthesis of 2,3-dihydroquinazolinones. The ESP of the catalyst is shown, in the plane of the CH and NH bonds for TS(E) and TS′(E), along with the atomic charges on the hydrogens and resulting electrostatic interaction ($E_{elec,}$ in kcal/mol). Adapted with permission from Ref. 35.

5.2 NHC Organocatalysis

NHCs are powerful organocatalysts capable of steering numerous challenging enantioselective transformations.[40] An early electrostatically guided example was provided by the Rovis and Houk groups' study on asymmetric intermolecular Stetter reactions,[41] where stereoselectivity could be modulated by strategically tuning the electrostatic environment surrounding the NHC catalyst. In a study of NHC-catalyzed [4+2] cycloadditions, Kozlowski, Bode, and coworkers[42] underscored the importance of an oxyanion steering mechanism that maximizes electrostatic interactions, while Scheidt, Cheong, and co-workers[30] and Schoenebeck, et al.[33] have documented similar effects.

Our foray into this area was directed toward understanding the role of protic additives and the origin of selectivity in NHC-catalyzed KRs. Across three disparate examples of KRs, together with one case of dynamic kinetic resolution (DKR), we identified electrostatic interactions as the universal driver of selectivity (reaction 8-11, Figure 8).[3] The stereoselectivities of these four reactions are dictated by hydrogen bonding networks with

markedly different features. For example, reaction 8 has a cyclic OH···O interaction that is distant from the critical bond-forming processes, whereas for reaction 9, the vital NH···O hydrogen bond is directly involved in the bond-forming/breaking step. Reaction 10 has a charge-assisted hydrogen bond (OH···O$^-$), whereas reaction 11 relies on the collective effects of three CH···O interactions that are again distant from the key bond-forming/breaking events in the TS. Despite these differences, all hydrogens involved in these charge-assisted hydrogen bond networks are in more favorable electrostatic environments in the TS structures leading to the major stereoisomer, providing a single electrostatic model that explains the observed selectivity in all four transformations. This can be seen in Figures 8b and 8c, where we quantify the electrostatic stabilization of the transferring proton in reactions 8 and 9, respectively.

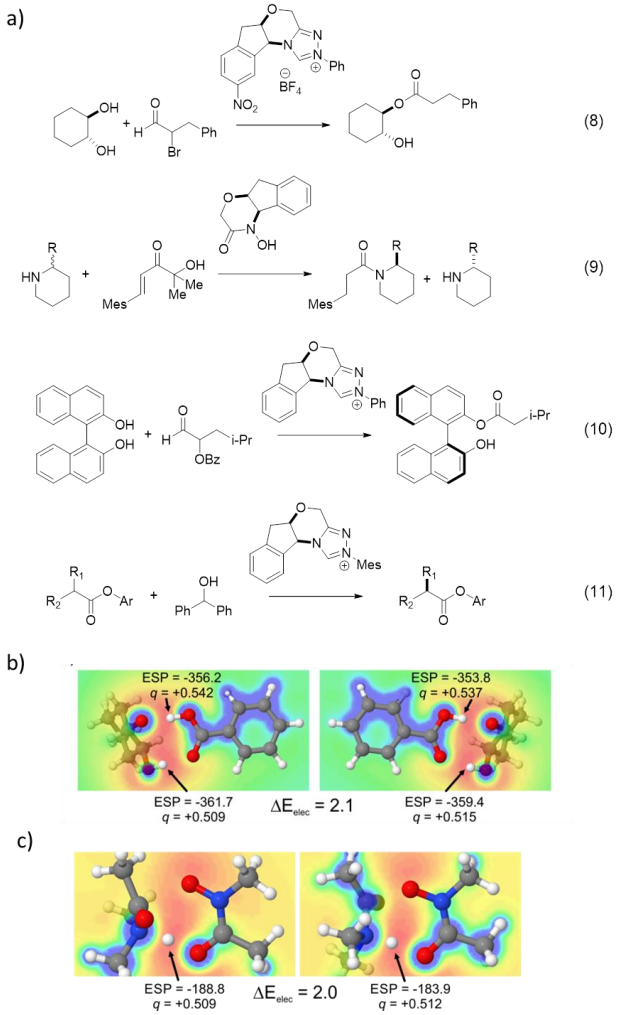

Figure 8. a) Three disparate NHC catalyzed KRs and one DKR; b) and c) quantifying the differences in electrostatic stabilization of the transferring proton in reaction 8 (b) and 9 (c). Adapted with permission from Ref. 3.

5.3 Counteranion Catalysis

Chiral counteranion catalysis, or asymmetric counterion-directed catalysis (ACDC), is a focal point for asymmetric method development,[43] yet our mechanistic understanding lags significantly behind ongoing methodological advances. This is presumably due at least in part to the large size of the catalysts, which places these systems at the limits of what can be readily handled with DFT. This complexity is further exacerbated when the counteranion lacks obvious substrate recognition sites, since there will be an enormous number of potential TS geometries varying in terms of the conformations of the substrate and catalyst as well as the precise arrangement of these species in the complex. We addressed one such challenge by studying[4] the asymmetric silylium ion-catalyzed Diels–Alder cycloaddition of cinnamate esters to cyclopentadiene (CP) from List and coworkers[44] (reaction 12, Figure 9). These reactions furnish high d.r. values (>25:1) for the *endo*-cycloadducts. In the stereocontrolling TS, we observed that ion pairing between the silylated cinnamate ester (the dienophile) and the chiral counterion catalyst (binaphthyl allyl tetrasulfone, BALT), creates a cleft that accommodates the reacting diene. In terms of diastereoselectivity, the conformation of the lowest-lying *exo*- and *endo*-TSs is similar, but with the CP rotated such that the ring is oriented differently within the cleft. Surprisingly, the gas-phase energy difference between these structures is primarily due to variation in non-covalent interaction energies, and analysis of truncated models revealed that this depends critically on the orientation of CP within the chiral electrostatic environment of the catalyst.

In the stereocontrolling TS structures the partial charges of the CP hydrogen atoms are not uniform, with the CH_2 hydrogens carry relatively more positive charge compared with their CH counterparts (see Figure 9b). Thus, different CP poses within the binding cleft lead to distinctive electrostatic environments for the methylene group, which enjoys greater stabilization in the *endo*-TS (due to electrostatically more favourable CH···O hydrogen bonds) than in the *exo*-TS. The proximity of a reacting counterion to a charged catalyst gives rise to strong electrostatic interactions that can differentiate stereodetermining transition states, in the case of a chiral catalyst.

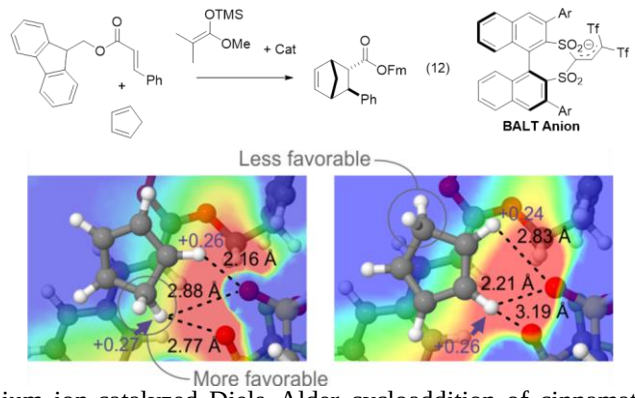

Figure 9. Asymmetric silylium ion-catalyzed Diels–Alder cycloaddition of cinnamate esters to cyclopentadiene. The ESP due to the catalyst and dienophile in the plane of key CP hydrogen atoms is shown for the endo (left) and exo (right) TS structures for one example, along with natural atomic charges for selected H atoms and interaction distances. Portions adopted with permission from Ref. 4.

6. Outlook

Through representative examples, we have illustrated electrostatic interactions as key drivers across a broad spectrum of organocatalytic reactions. Until recently, computational analysis of electrostatic interactions in catalysis was often relegated to the role of rationalizing experimental results retrospectively, rather than being applied predictively. As the field has matured, this approach has increasingly been embraced as a design element, giving a deeper understanding of electrostatic interactions and advancing rational catalyst design. By challenging earlier paradigms, enhanced reactivity and selectivity have been realized for many synthetic transformations using *in silico* methods. In a remarkable example of computationally guided discovery,[45] Cheong, Scheidt, and coworkers harnessed the power of electrostatic interactions to design imidazolium-based *N*-heterocyclic carbene (NHC) catalysts for asymmetric homoenolate additions of α-ketophosphonates. They exploited a critical nonclassical hydrogen bond between the aryl proton and phosphoryl oxygen in the stereodetermining step to devise a more selective catalyst. Introducing *m*-substituents on the terminal NHC phenyl group disrupted stabilizing CH···O interactions in the TS leading to the minor stereoisomer, enhancing enantioselectivity.

The impact of electrostatic interactions on reactivity and selectivity transcends the area of organocatalysis, with crucial involvement also documented in metal catalysis, Lewis acid catalysis, photoredox catalysis, supramolecular catalysis, and biocatalysis. In organometallic catalysis, Schoenebeck and coworkers[46] leveraged the electronegativity of CF_3 substituents when designing a ligand to trigger the demanding reductive elimination of $ArCF_3$ from Pd(II), by inducing electrostatic repulsion of the "leaving" CF_3 group. In a major success story of

computationally guided design, Head-Gordon and coworkers recently improved[47] the efficiency of a *de novo* designed Kemp eliminase enzyme by modulating the local electrostatic environment in the active site. Such examples attest to the potential of computationally directed design based on electrostatics.

Despite this considerable promise, the full power of electrostatically driven reactivity is yet to be fully harnessed. Here we highlight untapped potential in three particular areas. First, molecular mechanics (MM) methods are routinely employed to computing electric fields within enzyme binding pockets, and the role of electric fields in steering biocatalystic reactions is well recognized. Similar analyses have rarely been applied to the realm of organocatalysts. However, many of the above discussions of electrostatic stabilization can be recast in the language of electric fields (the electric field is the negative of the gradient of the ESP at that position). For instance, while we discussed Matile's anion-π catalyzed Kemp elimination in terms of the stabilization of negative charge by the ESP due to the NDI (Figure 2), you could instead consider the movement of the proton relative to the electric field created by the NDI. In the case of the original catalyst (**1**), the proton is moving in a region of minimal electric field strength, whereas in the redesigned catalyst (**2**) there is a strong electric field that will drive the proton from the substrate to the carboxylate, and hence accelerate the reaction.

Second, current experimental endeavors in catalysis rely on the stabilization of the TS by a preinstalled and permanently charged motif in the substrate or catalyst, limiting reaction scope. As the field advances, it will be possible to design catalysts with transient electrostatic directing groups, or even to tune the electrostatic environments distant from the catalytic center. Despite the conceptual complexity involved, recent efforts by the Phipps[48] group have provided a significant step forward in this direction.

Finally, integration of these fundamental learnings with data science and machine learning may constitute another force for innovation, as exemplified by the use of secondary-sphere electrostatic interactions to fine-tune organocatalyst reactivity by Milo and coworkers.[49] Such strategies will be particularly useful for the rational design of organocatalysts, given the high computational demand associated with their large size and flexibility.[50] Our efforts to design catalysts for asymmetric propargylations through automated quantum chemical predictions[51] has shown that enhanced selectivity can be achieved by modulating the ESP in the region of the formyl CH group of benzaldehyde (see Figure 2) through the judicious fluorine

substitution on the catalyst. Such emerging techniques offer a new frontier for reaction discovery.

We hope that the underlying principles of electrostatic interaction described in this review will encourage a deeper appreciation of their relevance in catalysis, paving the way for future design of new reactions and catalysts to solve outstanding synthetic challenges.

Acknowledgments

We thank T.J. Seguin, T. Liu, A. C. Doney, M. A. Porterfield, and C.J. Laconsay for their invaluable contributions.

Biographical Information

Rajat Maji graduated from IIT-Kharagpur and earned his Ph.D. in computational organic chemistry from Texas A&M working under Prof. Steven Wheeler. He relocated to Germany to work in the laboratory of Prof. Benjamin List (Max-Planck-Institut für Kohlenforschung), as a Marie Sklodowska-Curie Fellow designing novel asymmetric organocatalytic hydrofunctionalizations. He is currently a postdoc at UCLA, under the direction of Prof. Abigail Doyle, exploring new avenues of photoredox catalysis and data science.

Sharath Chandra Mallojjala obtained his undergraduate degree in the sciences from IISER-Pune in 2015. He joined the Wheeler Group at Texas A&M in the Fall of 2015 and subsequently transferred to the Center for Computational Quantum Chemistry (CCQC) at the University of Georgia (UGA) in 2017, obtaining his Ph.D. in 2019. He is currently a postdoc in the Hirschi group at SUNY Binghamton, working on isotope effects and computational biocatalysis.

Steven E. Wheeler graduated from New College of Florida in 2002 and completed his Ph.D. in 2006 at the University of Georgia. He was a postdoc in Ken Houk's group at UCLA before joining the faculty at Texas A&M in 2010. He was promoted to associate professor in 2015 and named Davidson Professor of Science in 2016. He returned to UGA in January, 2017, and was promoted to full professor in 2021. He spends most waking hours thinking deeply about stacking interactions.

References

(1) Maji, R.; Ugale, H.; Wheeler, S. E. Understanding the Reactivity and Selectivity of Fluxional Chiral DMAP-Catalyzed Kinetic Resolutions of Axially Chiral Biaryls. *Chemistry – A European Journal* **2019**, *25* (17), 4452-4459. DOI: https://doi.org/10.1002/chem.201806068.

(2) Maji, R.; Champagne, P. A.; Houk, K. N.; Wheeler, S. E. Activation Mode and Origin of Selectivity in Chiral Phosphoric Acid-Catalyzed Oxacycle Formation by Intramolecular Oxetane Desymmetrizations. *ACS Catalysis* **2017**, *7* (10), 7332-7339. DOI: 10.1021/acscatal.7b02993.

(3) Maji, R.; Wheeler, S. E. Importance of Electrostatic Effects in the Stereoselectivity of NHC-Catalyzed Kinetic Resolutions. *Journal of the American Chemical Society* **2017**, *139* (36), 12441-12449. DOI: 10.1021/jacs.7b01796.

(4) Seguin, T. J.; Wheeler, S. E. Stacking and Electrostatic Interactions Drive the Stereoselectivity of Silylium-Ion Asymmetric Counteranion-Directed Catalysis. *Angew. Chem. Int. Ed.* **2016**, *55* (51), 15889-15893. DOI: 10.1002/anie.201609095.

(5) Herbert, J. M. Neat, Simple, and Wrong: Debunking Electrostatic Fallacies Regarding Noncovalent Interactions. *J Phys Chem A* **2021**, *125* (33), 7125-7137. DOI: 10.1021/acs.jpca.1c05962.

(6) Kennedy, C. R.; Lin, S.; Jacobsen, E. N. The Cation–π Interaction in Small-Molecule Catalysis. *Angewandte Chemie International Edition* **2016**, *55* (41), 12596-12624. DOI: https://doi.org/10.1002/anie.201600547.

(7) Zhao, Y.; Cotelle, Y.; Liu, L.; López-Andarias, J.; Bornhof, A.-B.; Akamatsu, M.; Sakai, N.; Matile, S. The Emergence of Anion−π Catalysis. *Accounts of Chemical Research* **2018**, *51* (9), 2255-2263. DOI: 10.1021/acs.accounts.8b00223.

(8) Wheeler, S. E.; Houk, K. N. Substituent effects in cation/pi interactions and electrostatic potentials above the centers of substituted benzenes are due primarily to through-space effects of the substituents. *J Am Chem Soc* **2009**, *131* (9), 3126-3127. DOI: 10.1021/ja809097r From NLM Medline. Wheeler, S. E.; Houk, K. N. Are anion/pi interactions actually a case of simple charge-dipole interactions? *J Phys Chem A* **2010**, *114* (33), 8658-8664. DOI: 10.1021/jp1010549 From NLM Medline.

(9) Wheeler, S. E.; Bloom, J. W. Anion-pi interactions and positive electrostatic potentials of N-heterocycles arise from the positions of the nuclei, not changes in the pi-electron distribution.

Chem Commun (Camb) **2014**, *50* (76), 11118-11121. DOI: 10.1039/c4cc05304d From NLM PubMed-not-MEDLINE.

(10) Bootsma, A. N.; Wheeler, S. E. Tuning Stacking Interactions between Asp-Arg Salt Bridges and Heterocyclic Drug Fragments. *J Chem Inf Model* **2019**, *59* (1), 149-158. DOI: 10.1021/acs.jcim.8b00563. Bootsma, A. N.; Wheeler, S. E. Converting SMILES to Stacking Interaction Energies. *J Chem Inf Model* **2019**, *59* (8), 3413-3421. DOI: 10.1021/acs.jcim.9b00379.

(11) Wheeler, S. E.; Houk, K. N. Through-Space Effects of Substituents Dominate Molecular Electrostatic Potentials of Substituted Arenes. *J Chem Theory Comput* **2009**, *5* (9), 2301-2312. DOI: 10.1021/ct900344g From NLM PubMed-not-MEDLINE.

(12) Johnston, R. C.; Cheong, P. H. C-H...O non-classical hydrogen bonding in the stereomechanics of organic transformations: theory and recognition. *Org Biomol Chem* **2013**, *11* (31), 5057-5064. DOI: 10.1039/c3ob40828k.

(13) Warshel, A.; Sharma, P. K.; Kato, M.; Xiang, Y.; Liu, H.; Olsson, M. H. M. Electrostatic Basis for Enzyme Catalysis. *Chemical Reviews* **2006**, *106* (8), 3210-3235. DOI: 10.1021/cr0503106.

(14) Nepal, B.; Scheiner, S. Effect of Ionic Charge on the CH···π Hydrogen Bond. *J. Phys. Chem. A* **2014**, *118* (40), 9575-9587. DOI: 10.1021/jp5070598.

(15) Mecozzi, S.; West, A. P., Jr.; Dougherty, D. A. Cation-pi interactions in aromatics of biological and medicinal interest: electrostatic potential surfaces as a useful qualitative guide. *Proc Natl Acad Sci U S A* **1996**, *93* (20), 10566-10571. DOI: 10.1073/pnas.93.20.10566.

(16) Espinosa, E.; Molins, E.; Lecomte, C. Hydrogen bond strengths revealed by topological analyses of experimentally observed electron densities. *Chemical Physics Letters* **1998**, *285* (3), 170-173. DOI: https://doi.org/10.1016/S0009-2614(98)00036-0.

(17) Li, Y.; He, C. Q.; Gao, F.-X.; Li, Z.; Xue, X.-S.; Li, X.; Houk, K. N.; Cheng, J.-P. Design and Applications of N-tert-Butyl Sulfinyl Squaramide Catalysts. *Organic Letters* **2017**, *19* (7), 1926-1929. DOI: 10.1021/acs.orglett.7b00727.

(18) Belding, L.; Taimoory, S. M.; Dudding, T. Mirroring Enzymes: The Role of Hydrogen Bonding in an Asymmetric Organocatalyzed Aza-Henry Reaction—a DFT Study. *ACS Catal.* **2015**, *5* (1), 343-349. DOI: 10.1021/cs501062u.

(19) Jeziorski, B.; Moszynski, R.; Szalewicz, K. Perturbation-Theory Approach to Intermolecular Potential-Energy Surfaces of Van-Der-Waals Complexes. *Chem. Rev.* **1994**, *94* (7), 1887-1930. DOI: DOI 10.1021/cr00031a008. Szalewicz, K. Symmetry-adapted perturbation theory of intermolecular forces. *Wiley Interdisciplinary Reviews-Computational Molecular Science* **2012**, *2* (2), 254-272. DOI: 10.1002/wcms.86. Hohenstein, E. G.; Sherrill, C. D. Density fitting of intramonomer correlation effects in symmetry-adapted perturbation theory. *J. Chem. Phys.* **2010**, *133* (1), 014101. DOI: 10.1063/1.3451077. Hohenstein, E. G.; Sherrill, C. D. Density fitting and Cholesky decomposition approximations in symmetry-adapted perturbation theory: Implementation and application to probe the nature of pi-pi interactions in linear acenes. *J. Chem. Phys.* **2010**, *132* (18), 184111. DOI: Artn 184111 10.1063/1.3426316.

(20) Parrish, R. M.; Sherrill, C. D. Spatial assignment of symmetry adapted perturbation theory interaction energy components: The atomic SAPT partition. *J Chem Phys* **2014**, *141* (4), 044115. DOI: 10.1063/1.4889855 From NLM PubMed-not-MEDLINE.

(21) Parrish, R. M.; Parker, T. M.; Sherrill, C. D. Chemical Assignment of Symmetry-Adapted Perturbation Theory Interaction Energy Components: The Functional-Group SAPT Partition. *J Chem Theory Comput* **2014**, *10* (10), 4417-4431. DOI: 10.1021/ct500724p From NLM PubMed-not-MEDLINE.

(22) Bakr, B. W.; Sherrill, C. D. Analysis of transition state stabilization by non-covalent interactions in organocatalysis: application of atomic and functional-group partitioned symmetry-adapted perturbation theory to the addition of organoboron reagents to fluoroketones. *Phys Chem Chem Phys* **2018**, *20* (27), 18241-18251. DOI: 10.1039/c8cp02029a From NLM PubMed-not-MEDLINE.

(23) Lee, K.; Silverio, D. L.; Torker, S.; Robbins, D. W.; Haeffner, F.; van der Mei, F. W.; Hoveyda, A. H. Catalytic enantioselective addition of organoboron reagents to fluoroketones controlled by electrostatic interactions. *Nat Chem* **2016**, *8* (8), 768-777. DOI: 10.1038/nchem.2523 From NLM Medline.

(24) Zhao, Y.; Domoto, Y.; Orentas, E.; Beuchat, C.; Emery, D.; Mareda, J.; Sakai, N.; Matile, S. Catalysis with anion-pi interactions. *Angew Chem Int Ed Engl* **2013**, *52* (38), 9940-9943. DOI: 10.1002/anie.201305356 From NLM PubMed-not-MEDLINE. Zhao, Y.; Beuchat, C.; Domoto,

Y.; Gajewy, J.; Wilson, A.; Mareda, J.; Sakai, N.; Matile, S. Anion-pi catalysis. *J Am Chem Soc* **2014**, *136* (5), 2101-2111. DOI: 10.1021/ja412290r From NLM Medline.

(25) Lu, T.; Wheeler, S. E. Quantifying the Role of Anion−π Interactions in Anion−π Catalysis. *Org. Lett.* **2014**, *16* (12), 3268-3271. DOI: 10.1021/ol501283u.

(26) Ma, G.; Deng, J.; Sibi, M. P. Fluxionally Chiral DMAP Catalysts: Kinetic Resolution of Axially Chiral Biaryl Compounds. *Angewandte Chemie International Edition* **2014**, *53* (44), 11818-11821. DOI: https://doi.org/10.1002/anie.201406684.

(27) de Freitas Martins, E.; Pliego, J. R. Unraveling the Mechanism of the Cinchoninium Ion Asymmetric Phase-Transfer-Catalyzed Alkylation Reaction. *ACS Catalysis* **2013**, *3* (4), 613-616. DOI: 10.1021/cs400021r.

(28) Lu, T.; Zhu, R.; An, Y.; Wheeler, S. E. Origin of Enantioselectivity in the Propargylation of Aromatic Aldehydes Catalyzed by Helical N-Oxides. *J. Am. Chem. Soc.* **2012**, *134* (6), 3095-3102. DOI: 10.1021/ja209241n.

(29) Lu, T.; Porterfield, M. A.; Wheeler, S. E. Explaining the Disparate Stereoselectivities of N-Oxide Catalyzed Allylations and Propargylations of Aldehydes. *Org. Lett.* **2012**, *14* (20), 5310-5313. DOI: 10.1021/ol302493d.

(30) Johnston, R. C.; Cohen, D. T.; Eichman, C. C.; Scheidt, K. A.; Ha-Yeon Cheong, P. Catalytic kinetic resolution of a dynamic racemate: highly stereoselective [small beta]-lactone formation by N-heterocyclic carbene catalysis. *Chemical Science* **2014**, *5* (5), 1974-1982, 10.1039/C4SC00317A. DOI: 10.1039/C4SC00317A.

(31) Yang, H.; Wong, M. W. Oxyanion Hole Stabilization by C–H···O Interaction in a Transition State—A Three-Point Interaction Model for Cinchona Alkaloid-Catalyzed Asymmetric Methanolysis of meso-Cyclic Anhydrides. *Journal of the American Chemical Society* **2013**, *135* (15), 5808-5818. DOI: 10.1021/ja4005893.

(32) Kótai, B.; Kardos, G.; Hamza, A.; Farkas, V.; Pápai, I.; Soós, T. On the Mechanism of Bifunctional Squaramide-Catalyzed Organocatalytic Michael Addition: A Protonated Catalyst as an Oxyanion Hole. *Chemistry – A European Journal* **2014**, *20* (19), 5631-5639. DOI: 10.1002/chem.201304553.

(33) Lyngvi, E.; Bode, J. W.; Schoenebeck, F. A computational study of the origin of stereoinduction in NHC-catalyzed annulation reactions of [small alpha],[small beta]-unsaturated

acyl azoliums. *Chemical Science* **2012**, *3* (7), 2346-2350, 10.1039/C2SC20331F. DOI: 10.1039/C2SC20331F.

(34) Maji, R.; Mallojjala, S. C.; Wheeler, S. E. Chiral phosphoric acid catalysis: from numbers to insights. *Chemical Society Reviews* **2018**, *47* (4), 1142-1158, 10.1039/C6CS00475J. DOI: 10.1039/C6CS00475J. Gao, S.; Duan, M.; Andreola, L. R.; Yu, P.; Wheeler, S. E.; Houk, K. N.; Chen, M. Unusual Enantiodivergence in Chiral Brønsted Acid-Catalyzed Asymmetric Allylation with β-Alkenyl Allylic Boronates. *Angewandte Chemie International Edition* **2022**, *61* (41), e202208908. DOI: https://doi.org/10.1002/anie.202208908. Seguin, T. J.; Lu, T.; Wheeler, S. E. Enantioselectivity in Catalytic Asymmetric Fischer Indolizations Hinges on the Competition of π-Stacking and CH/π Interactions. *Org. Lett.* **2015**, *17*, 3066-3069. Seguin, T. J.; Wheeler, S. E. Electrostatic Basis for Enantioselective Brønsted-Acid-Catalyzed Asymmetric Ring Openings of meso-Epoxides. *ACS Catalysis* **2016**, *6* (4), 2681-2688. DOI: 10.1021/acscatal.6b00538. Nimmagadda, S. K.; Mallojjala, S. C.; Woztas, L.; Wheeler, S. E.; Antilla, J. C. Enantioselective Synthesis of Chiral Oxime Ethers: Desymmetrization and Dynamic Kinetic Resolution of Substituted Cyclohexanones. *Angewandte Chemie International Edition* **2017**, *56* (9), 2454-2458. DOI: https://doi.org/10.1002/anie.201611602.

(35) Laconsay, C. J.; Seguin, T. J.; Wheeler, S. E. Modulating Stereoselectivity through Electrostatic Interactions in a SPINOL-Phosphoric Acid-Catalyzed Synthesis of 2,3-Dihydroquinazolinones. *ACS Catalysis* **2020**, *10* (20), 12292-12299. DOI: 10.1021/acscatal.0c02578.

(36) Parmar, D.; Sugiono, E.; Raja, S.; Rueping, M. Complete Field Guide to Asymmetric BINOL-Phosphate Derived Brønsted Acid and Metal Catalysis: History and Classification by Mode of Activation; Brønsted Acidity, Hydrogen Bonding, Ion Pairing, and Metal Phosphates. *Chem. Rev.* **2014**, *114*, 9047-9153.

(37) Sorgenfrei, N.; Hioe, J.; Greindl, J.; Rothermel, K.; Morana, F.; Lokesh, N.; Gschwind, R. M. NMR Spectroscopic Characterization of Charge Assisted Strong Hydrogen Bonds in Brønsted Acid Catalysis. *Journal of the American Chemical Society* **2016**, *138* (50), 16345-16354. DOI: 10.1021/jacs.6b09243.

(38) Wang, Z.; Law, W. K.; Sun, J. Chiral Phosphoric Acid Catalyzed Enantioselective Desymmetrization of *meso*-Epoxides by Thiols. *Org. Lett.* **2013**, *15*, 5964-5966.

(39) Seguin, T. J.; Wheeler, S. E. Electrostatic Basis of Asymmetric Ring Openings of meso-Epoxides. *ACS Catal.* **2016**, *6*, 2681-2688.
(40) Flanigan, D. M.; Romanov-Michailidis, F.; White, N. A.; Rovis, T. Organocatalytic Reactions Enabled by N-Heterocyclic Carbenes. *Chemical Reviews* **2015**, *115* (17), 9307-9387. DOI: 10.1021/acs.chemrev.5b00060.
(41) DiRocco, D. A.; Noey, E. L.; Houk, K. N.; Rovis, T. Catalytic Asymmetric Intermolecular Stetter Reactions of Enolizable Aldehydes with Nitrostyrenes: Computational Study Provides Insight into the Success of the Catalyst. *Angewandte Chemie International Edition* **2012**, *51* (10), 2391-2394. DOI: 10.1002/anie.201107597.
(42) Allen, S. E.; Mahatthananchai, J.; Bode, J. W.; Kozlowski, M. C. Oxyanion Steering and CH−π Interactions as Key Elements in an N-Heterocyclic Carbene-Catalyzed [4 + 2] Cycloaddition. *Journal of the American Chemical Society* **2012**, *134* (29), 12098-12103. DOI: 10.1021/ja302761d.
(43) Mahlau, M.; List, B. Asymmetric Counteranion-Directed Catalysis: Concept, Definition, and Applications. *Angewandte Chemie International Edition* **2013**, *52* (2), 518-533. DOI: https://doi.org/10.1002/anie.201205343.
(44) Gatzenmeier, T.; van Gemmeren, M.; Xie, Y.; Höfler, D.; Leutzsch, M.; List, B. Asymmetric Lewis acid organocatalysis of the Diels–Alder reaction by a silylated C–H acid. *Science* **2016**, *351* (6276), 949-952. DOI: 10.1126/science.aae0010.
(45) Jang, K. P.; Hutson, G. E.; Johnston, R. C.; McCusker, E. O.; Cheong, P. H. Y.; Scheidt, K. A. Asymmetric Homoenolate Additions to Acyl Phosphonates through Rational Design of a Tailored N-Heterocyclic Carbene Catalyst. *Journal of the American Chemical Society* **2014**, *136* (1), 76-79. DOI: 10.1021/ja410932t.
(46) Nielsen, M. C.; Bonney, K. J.; Schoenebeck, F. Computational Ligand Design for the Reductive Elimination of ArCF3 from a Small Bite Angle PdII Complex: Remarkable Effect of a Perfluoroalkyl Phosphine. *Angewandte Chemie International Edition* **2014**, *53* (23), 5903-5906. DOI: 10.1002/anie.201400837.
(47) Vaissier, V.; Sharma, S. C.; Schaettle, K.; Zhang, T.; Head-Gordon, T. Computational Optimization of Electric Fields for Improving Catalysis of a Designed Kemp Eliminase. *ACS Catalysis* **2018**, *8* (1), 219-227. DOI: 10.1021/acscatal.7b03151.

(48) Proctor, R. S. J.; Colgan, A. C.; Phipps, R. J. Exploiting attractive non-covalent interactions for the enantioselective catalysis of reactions involving radical intermediates. *Nature Chemistry* **2020**, *12* (11), 990-1004. DOI: 10.1038/s41557-020-00561-6.

(49) Dhayalan, V.; Gadekar, S. C.; Alassad, Z.; Milo, A. Unravelling mechanistic features of organocatalysis with in situ modifications at the secondary sphere. *Nature Chemistry* **2019**, *11* (6), 543-551. DOI: 10.1038/s41557-019-0258-1.

(50) Schreyer, L.; Properzi, R.; List, B. IDPi Catalysis. *Angewandte Chemie International Edition* **2019**, *58* (37), 12761-12777. DOI: 10.1002/anie.201900932.

(51) Doney, A. C.; Rooks, B. J.; Lu, T.; Wheeler, S. E. Design of Organocatalysts for Asymmetric Propargylations through Computational Screening. *ACS Catalysis* **2016**, *6* (11), 7948-7955. DOI: 10.1021/acscatal.6b02366.